Yatsyshin, P., Parry, A. O., Rascón, C., Kalliadasis, S. (2017). Wetting of a plane with a narrow solvophobic stripe. *Molecular Physics*, 116(15-16), pp. 1990-1997.

DOI: https://doi.org/10.1080/00268976.2018.1473648

Wetting of a plane with a narrow solvophobic stripe

P. Yatsyshin[a], A. O. Parry[b], C. Rascón[c] and S. Kalliadasis[a]

[a]Department of Chemical Engineering, Imperial College London, London, UK; [b]Department of Mathematics, Imperial College London, London, UK; [c]GISC, Universidad Carlos III de Madrid, Madrid, Spain

ABSTRACT

We present a numerical study of a simple Density Functional Theory model of fluid adsorption occurring on a planar wall decorated with a narrow deep stripe of a weaker adsorbing (relatively solvophobic) material, where wall-fluid and fluid-fluid intermolecular forces are considered to be dispersive. Both the stripe and outer sub-strate exhibit first-order wetting transitions with the wetting temperature of the stripe lying above that of the outer material. This geometry leads to a rich phase diagram due to the interplay between the pre-wetting transition of the outer sub-strate and an unbending transition corresponding to the local evaporation of liquid near the stripe. Depending on the width of the stripe the line of unbending transi-tions merges with the pre-wetting line inducing a 2D wetting transition occurring across the substrate. In turn, this leads to the continuous pre-drying of the thick pre-wetting film as the pre-wetting line is approached from above. Interestingly we find that the merging of the unbending and pre-wetting lines occurs even for the widest stripes considered. This contrasts markedly with the scenario where the outer material has the higher wetting temperature, for which the merging of the unbending and pre-wetting lines only occurs for very narrow stripes.

KEYWORDS

Wetting; classical density functional theory

1. Introduction

The resurgence of interest in wetting in the last few decades began with the recognition that this constituted a new example of a surface phase transition which could be of first or second-order [1–3]. Quickly it became apparent that continuous wetting transitions were extremely sensitive to the interplay between fluctuation effects, dimensionality and intermolecular forces leading to a rich variety of universality classes and fluctuation regimes [4–7] - see for example the comprehensive reviews [8–10]. It was also recognized that wetting plays an important role in determining the quantitative and qualitative aspects of fluid adsorption in capillary slit (parallel plate) geometries [11, 12]. This is particularly important when the walls are competing for which respective wetting and drying properties determine completely the nature of the interfacial delocalization and drive the allowed phase coexistence and criticality [13, 14]. In all of these studies Density Functional Theory (DFT) has proved a valuable tool for investigating the

CONTACT P. Yatsyshin. Email: p.yatsyshin@imperial.ac.uk

phase equilibria and also correlation function structure at a microscopic level [15, 16] and complements other approaches for example those based on mesoscopic interfacial models - again see [10] for a comprehensive review.

More recently attention has focused on more complex geometries such as wedges [17–20], capped capillaries (capillary grooves) [21–24] and other geometries [25–28] where wetting competes with other phase transitions such as filling and capillary condensation to induce further examples of interfacial phase transitions. These fundamental studies of fluid adsorption are further motivated by the fact that adsorption at the nanoscale is important in many technological processes, including the design of lab-on-a-chip devices, superhydrophobic surfaces and the burgeoning field of nanofluidics [29–36]. Returning to the more fundamental statistical mechanical issues, it is now apparent that even relatively simple confining geometries can produce very rich phase diagrams due to the competition between different phase transitions [37] – these more subtle issues go beyond the classical concepts of Cassie-Baxter and Wenzel states of sessile drops on rough and patterned surfaces.

An example of this is the fluid adsorption occurring on a planar substrate decorated with a stripe of a different material. In a recent paper we investigated this for the case in which the stripe has stronger preferential adsorption of liquid, i.e. is relatively solvophillic compared to the outer substrate [38]. In this case the pre-wetting transition of the outer substrate competes with a local surface condensation (unbending) transition occurring near the stripe. Two effects emerge from this; first, the local nucleation of liquid near the stripe leads to phenomena of complete prewetting, a 2D surface phase transition occurring across substrate as the pre-wetting line (of the outer wall) is approached from below [39, 40]. The possibility of this transition was overlooked in earlier studies of wetting on similarly patterned walls [37, 41–43]. Secondly, when the width L of the stripe is very small, of order ten molecular diameters, the line of unbending transition merges with the pre-wetting line which in turn leads to a new 2D wetting transition also occurring along the substrate.

In the present paper we study the reverse scenario where the material of the stripe is weaker, i.e. relatively solvophobic, so that its wetting temperature is higher than that of the outer wall. In this case we can similarly expect complete pre-wetting will occur, but now as a film of low density gas which spreads out along the wall from the stripe as the pre-wetting line (again of the outer wall) is approached from *above*. However just because the strength of the inner and outer regions are flipped, this does not imply that surface phase diagrams are simple mirror images; the bulk phase remains gas in both cases but now the outer wall becomes completely wet as bulk coexistence is approached. We shall show that this has a very strong influence on the possible merging of the pre-wetting and unbending lines.

2. Density functional model and methodology

As mentioned above, our methodology is based on classical DFT, and follows closely our previous work, discussed in further detail in reference [38]. All intermolecular interactions are given by the Lennard-Jones (LJ) potential with well depth ε and range σ:

$$\varphi^{\mathrm{LJ}}_{\sigma,\varepsilon}(r) = 4\varepsilon\left[\left(\frac{\sigma}{r}\right)^{12} - \left(\frac{\sigma}{r}\right)^{6}\right]. \tag{1}$$

Consider a flat wall of material type (w), whose adatoms exert a potential $\varphi^{\mathrm{LJ}}_{\sigma_{\mathrm{w}},\varepsilon_{\mathrm{w}}}(r)$ on the fluid molecules. For such a wall, located in the plane $y = 0$, the cumulative potential acting on the fluid is obtained by integrating $\varphi^{\mathrm{LJ}}_{\sigma_{\mathrm{w}},\varepsilon_{\mathrm{w}}}(r)$ over the volume of the wall:

$$V_0(y) = 4\pi\rho_{\mathrm{w}}\varepsilon_{\mathrm{w}}\sigma_{\mathrm{s}}^3\left[-\frac{1}{6}\left(\frac{\sigma_{\mathrm{w}}}{H_0+y}\right)^3 + \frac{1}{45}\left(\frac{\sigma_{\mathrm{w}}}{H_0+y}\right)^9\right], \tag{2}$$

where ρ_{w} is the average density of the material (w) and H_0 is a near-wall cut-off, introduced to avoid a non-physical divergence of $V_0(y)$ at contact with the fluid. The effect of varying the finite $H_0 > 0$ on planar wetting is investigated in, e.g., Appendix 1 of Reference [44], where it is shown that such low-y cut-off does not qualitatively affect the wetting phenomenology.

When a macroscopically deep stripe of material type (s) of width L with the pairwise fluid-substrate potential $\varphi^{\mathrm{LJ}}_{\sigma_{\mathrm{s}},\varepsilon_{\mathrm{s}}}(r)$ is inserted into the wall, the total potential of the decorated substrate is modified to

$$V_L(x,y) = V_0(y) - \rho_{\mathrm{w}}\int_{\nu_L} \mathrm{d}\mathbf{r}'\ \varphi^{\mathrm{LJ}}_{\sigma_{\mathrm{w}},\varepsilon_{\mathrm{w}}}\left(\left|\mathbf{r}-\mathbf{r}'\right|\right) + \rho_{\mathrm{s}}\int_{\nu_L} \mathrm{d}\mathbf{r}'\ \varphi^{\mathrm{LJ}}_{\sigma_{\mathrm{s}},\varepsilon_{\mathrm{s}}}\left(\left|\mathbf{r}-\mathbf{r}'\right|\right), \tag{3}$$

where the integration is carried out over the volume ν_L of the stripe, excluding the coating: $\nu_L = \{(x,y,z) : -L/2 \le x \le L/2, -\infty < y \le -H_0, -\infty < z < \infty\}$. Clearly, $V_{L=0}(x,y) \equiv V_0(y)$, and $V_{L\to\infty}(y)$ is the potential of a homogeneous wall made up of material (s). Translational invariance is assumed in the z direction.

The density profile $\rho(\mathbf{r})$ of the fluid, adsorbed on a striped wall at temperature T and chemical potential μ, can be obtained by unconstrained numerical minimization of the grand free energy functional [15, 16, 45, 46]:

$$\Omega[\rho(\mathbf{r})] = F[\rho(\mathbf{r})] - \int \mathrm{d}\mathbf{r}\ \rho(\mathbf{r})\left(\mu - V_L(x,y)\right). \tag{4}$$

Here $F[\rho(\mathbf{r})]$ is the intrinsic Helmholtz free energy functional, for which we use a simple local density approximation to model the hard sphere contribution, together with a mean-field treatment of the attractive forces [16]:

$$\begin{aligned} F[\rho(\mathbf{r})] \quad &= \int \mathrm{d}\mathbf{r}\ \left[\, f_{\mathrm{id}}(\rho(\mathbf{r})) + \rho(\mathbf{r})\,\psi(\rho(\mathbf{r}))\,\right] \\ &\quad + \tfrac{1}{2}\int \mathrm{d}\mathbf{r}\int \mathrm{d}\mathbf{r}'\ \rho(\mathbf{r})\,\rho(\mathbf{r}')\,\varphi_{\mathrm{attr}}\left(|\mathbf{r}-\mathbf{r}'|\right), \end{aligned} \tag{5}$$

where $f_{\mathrm{id}}(\rho) = k_{\mathrm{B}}T\rho\left(\ln\left(\lambda^3\rho\right) - 1\right)$ is the free energy density of ideal gas (λ is the thermal de Broigle wavelength), and $\psi(\rho)$ is the Carnahan-Starling free energy density of a gas of hard spheres of radius σ:

$$\psi(\rho) \ = \ k_{\mathrm{B}}T\ \frac{\eta(4-3\eta)}{(1-\eta)^2}, \qquad \eta = \pi\sigma^3\rho/6. \tag{6}$$

The attractive part of the fluid intermolecular interaction $\varphi_{\mathrm{attr}}(|\mathbf{r}-\mathbf{r}'|)$ closely follows

the Barker-Henderson approximation[47]:

$$\varphi_{\mathrm{attr}}(r) = \begin{cases} 0, & r \leq \sigma \\ \varphi^{\mathrm{LJ}}_{\sigma,\varepsilon}(r), & r > \sigma. \end{cases} \tag{7}$$

In the uniform limit, the approximation for $F[\rho(\mathbf{r})]$ of the Lennard-Jones (LJ) fluid free energy in Equation (5) is equivalent to the random phase approximation of the bulk pair correlation function [16]. Although the local treatment of repulsive interactions does not recover the oscillatory behaviour and layering when a high-density liquid is near a substrate, we do not anticipate that this affects the qualitative aspects of the new phase transitions occurring on the decorated substrate considered here.

To proceed we define the adsorption on the striped wall relative to the homogeneous (w)-wall:

$$\Gamma = \int_{-\infty}^{\infty} dx \int_{0}^{\infty} dy \; [\rho_L(x,y) - \rho_{L=0}(y)], \tag{8}$$

where $\rho_L(x,y)$ and $\rho_{L=0}(y)$ are the respective fluid density profiles near the wall with and without the stripe, computed at the same values of T and μ. The excess grand potential, which is the thermodynamic conjugate to the adsorption, is given by

$$\Omega_{\mathrm{ex}} = \Omega[\rho_L(x,y)] - \Omega[\rho_{L=0}(y)], \tag{9}$$

and obeys the surface Gibbs adsorption equation:

$$\Gamma(\mu) = -\frac{1}{\mathcal{L}} \left(\frac{\partial \Omega_{\mathrm{ex}}}{\partial \mu} \right)_T, \tag{10}$$

where $\mathcal{L}$ is the system's transverse dimension along the z-axis.

In the present mean-field analysis, phase coexistence is associated, as per usual, with hysterisis loops for the adsorption isotherms $\Gamma(\mu)$. Thus, the coexisting fluid phases (i.e., configurations $\rho(x,y)$ whose grand potentials are equal) are associated with a generalized Maxwell equal area construction imposed on the hysteresis loops of the adsorption isotherms. This allows us to perform a fully consistent mean-field analysis. Further details on the approximations involved in (4)–(7), as well as full details of the numerical scheme, used to minimize the grand free energy functional and trace the full isotherms can be found elsewhere [28, 44, 48].

3. Results and discussion

For the computations presented here we use the hard core diameter σ and the well depth ε of the fluid–fluid LJ interactions as the units of length and energy, respectively. In these units the bulk critical temperature of the LJ fluid occurs at $T_{\mathrm{c}} \approx 1.006$. Without loss of generality, we further set $\rho_{\mathrm{w}} = \rho_{\mathrm{s}} = 1$ and $H_0 = 5$ in (2) and (3), and fix the values of the parameters of the wall (w) and stripe (s) materials to $\varepsilon_{\mathrm{w}} = 0.8$, $\varepsilon_{\mathrm{s}} = 0.6$ and $\sigma_{\mathrm{w}} = \sigma_{\mathrm{s}} = 2$. This separates the wetting temperatures of the inner and outer substrates, allowing us to identify a temperature regime where the stripe is relatively solvophobic, compared to the outer material, see figure 1. As mentioned above, our

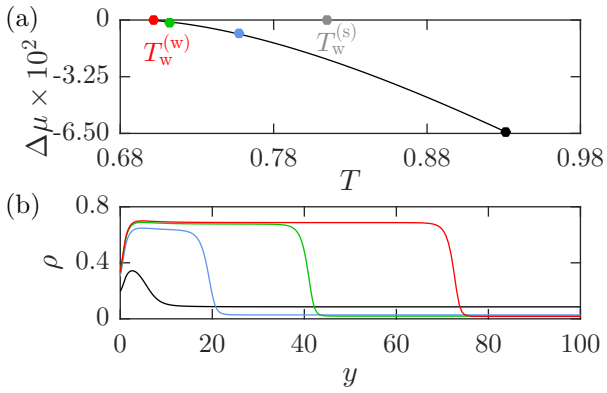

Figure 1. Phase diagram (a) and representative adsorption density profiles (b) for a homogeneous wall of material type (w). A first-order wetting trasition occurs at temperature $T_w^{(w)} \approx 0.70$ (red circle) and the line of pre-wetting terminates at a critical point $T_{pw,\,c}^{(w)} \approx 0.93$ (black circle). Also shown for reference is the location of the wetting temperature for the homogeneous substrate of material type (s), which occurs at the higher temperature $T_w^{(s)} \approx 0.81$ (grey circle). The representative density profiles in (b) correspond to the coexisting thick pre-wetting films at the points indicated in (a).

analysis of the phase behaviour is based on a standard thermodynamic method of van der Waals loops, with the control parameters being temperature T and chemical potential μ. Since we are investigating a scenario where the stable bulk thermodynamic phase is gas, it is most convenient to plot isotherms and phase diagrams in the T–$\Delta\mu$ plane, where $\Delta\mu\,(T) = \mu - \mu_{sat} \leq 0$ is the deviation of the chemical potential from the saturation value μ_{sat}.

3.1. The homogeneous planar wall

To begin, we first compute the surface phase diagram for a homogeneous wall of material type (w), described by the potential in Equation (2). The computed phase diagram is shown in Figure 1(a). The pre-wetting line $\Delta\mu_{pw}^{(w)}\,(T)$ approaches bulk coexistence ($\Delta\mu = 0$) tangentially, as expected, at a wetting temperature identified numerically as $T_w^{(w)} \approx 0.70$. Note, that since $\varepsilon_w < \varepsilon_s$, the wetting temperature of the homogeneous (s)-wall is higher, occurring at $T_w^{(s)} \approx 0.81 > T_w^{(w)}$, which is shown for comparison. Figure 1(b) shows a set of representative density profiles corresponding to the thick pre-wetting films at different temperatures along the pre-wetting line. As can be seen, these profiles have near-constant plateaus of density near the values of the bulk coexisting liquid and gas densities. As coexistence is approached (along the pre-wetting line) it is apparent that the thickness of the wetting layer of liquid diverges. Near saturation the thickness of the adsorbed liquid film grows according to the expected Derjaguin law $\mathcal{O}(\Delta\mu)^{-1/3}$ where the exponent is specific to the $\mathcal{O}(r^{-6})$ tail of the LJ forces. We have also checked that close to saturation the pre-wetting line is described by the expected asymptotic law $T - T_w \propto (\Delta\mu)^{3/2}$, and therefore merges with the saturation line tangentially.

3.2. Heterogeneous wall with a solvophobic stripe

Surface phase diagrams for a wall with a solvophobic stripe, corresponding to four different widths, are shown in Figure 2. The black line corresponds to the pre-wetting

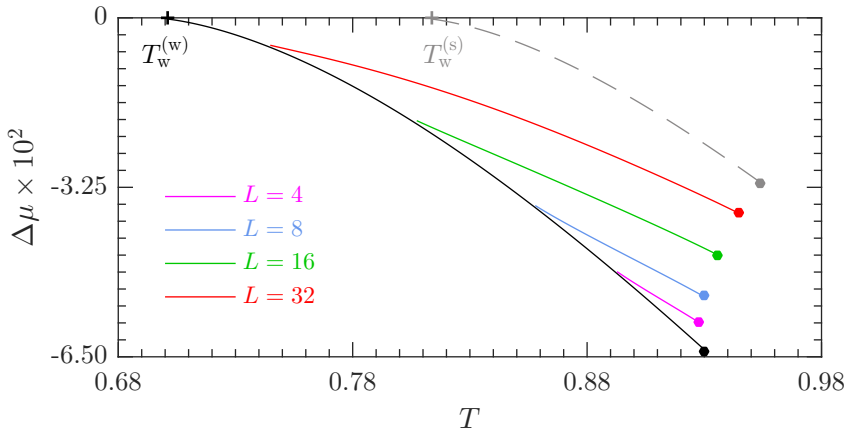

Figure 2. Surface phase diagrams for fluid adsorption near a solvaphobic stripe for different stripe width L. Pre-wetting lines prew-wetting lines for uniform (w)-wall (solid black) and (s)-wall (dashed grey) are shown together with the unbending lines, the locations of which are different for the different widths. The pre-wetting lines approach the bulk coexistence line $\Delta\mu = 0$ tangentially and similarly each unbending line merges with the pre-wetting line tangentially. The respective temperatures T^* at which the lines merge occur at $T^* \approx 0.89$, 0.86, 0.81 and 0.75 and approach the pre-wetting critical point as the width decreases.

line of the outer wall of material type (w), location of which is, of course, unchanged from that shown in Figure 1 for the homogeneous (w) wall. For reference we also show the pre-wetting line of the homogeneous (s) wall (grey dashed) which lies at considerably higher temperatures. For each strip width L a line of unbending phase transitions extends away from the pre-wetting line ending in a pre-wetting critical point. The line of unbending transitions always merges tangentially with the pre-wetting line with the temperature T^* at which these lines merge approaching the pre-wetting critical point as the width L is reduced.

Each phase diagram illustrates a number of distinct surface phase transitions. As the pre-wetting line is approached from below, a first-order thin-thick phase transition occurs, very similar to that occurring at a planar wall of type (w). The pre-wetting transition is also first-order when approached from above for temperatures T which lie below T^*. However when $T > T^*$ the pre-wetting transition is continuous when the pre-wetting line is approached from above. In this case the solvophopic stripe is on each side wet by a layer of the "thinner" pre-wetting phase, the size of which grows, spreading laterally away from the stripe, as we approach the pre-wetting line. This means the relative adsorption Γ is negative and diverges continuously similar to a 2D complete wetting transition occurring across the substrate. The divergence of the adsorption along an isotherm lying above $T*$ is shown in Figure 3 for a narrow stripe, with $L = 4$, where it is compared to the theoretical prediction $\Gamma \propto (\mu - \mu_{\rm pw})^{-\frac{1}{4}}$ [40]. Density profiles illustrating this will be discussed later. This example of complete pre-wetting is the converse of what happens for a solvophillic stripe, which nucleates the thicker pre-wetting phase, the lateral size of which grows as the pre-wetting line is approached from below. The temperature T^* must therefore correspond to a 2D wetting transition occurring in the $x-z$ plane. This transition is first-order at mean-field level, although fluctuation effects associated with the unbinding thin-thick interface, must alter this to continuous when the thermal wandering is allowed for.

The striped substrate also induces an unbending transition corresponding to the local condensation of liquid near the stripe. The line of unbending transitions meets the pre-wetting line tangentially at T^*, analogous to the merging of the pre-wetting

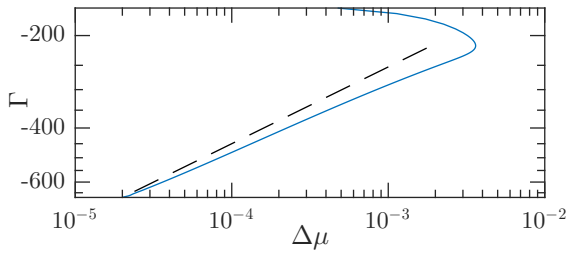

Figure 3. Adsorption isotherm, at $T = 0.80$ for a wall with a stipe of width $L = 4$, showing the continuous divergence of the adsorption (complete pre-wetting), as the pre-wetting line is approached from above. In this limit a gas-like film of the thinner pre-wetting phase spreads out laterally across the substrate (that is, in the x direction), away from the stripe. The dashed line is a guide to the eye, corresponding to the expected asymptotic divergence $\Gamma(\mu) \propto (\mu_{\rm pw} - \mu)^{-1/4}$.

and bulk saturation curves – this again reflects the first-order nature of the 2D wetting transition occurring at T^*. Theoretical considerations based on mesoscopic interfacial models predict that $\mathcal{O}\left(\mu - \mu_{\rm pw}\right)^{-1/4}$, with $\mu \to \mu_{\rm pw}$, which is quantitatively different to the merging of the pre-wetting and saturation lines, due to the reduced dimensionality of the wetting transition occurring at T^* and reflects the $-1/4$ power-law characterizing the divergence of $\Gamma(\mu)$ for the complete pre-wetting. Isotherms for unbending transition and representative coexisting profiles are shown in Figures 4 and 5.

Figure 4(a) shows characteristic adsorption isotherms for three different temperatures $T = 0.85$, 0.88 and 0.93 for a stripe of width $L = 8$. At $T = 0.88$ a prominent hysteresis loop in $\Gamma\left(\mu\right)$ is apparent, and a Maxwell equal areas construction determines the value of chemical potential at which the unbending transition occurs. The density profiles of the coexisting fluid configurations are represented in Figure 4(b), and demonstrate the local drying of the thick pre-wetting film, caused by the stripe. The isotherm at $T = 0.93$ corresponds to the limit where the hysteresis loop vanishes, corresponding therefore to the unbending critical point. The critical density profile is given in Figure 4(c) and illustrates the narrowing of the dry region at this higher temperature. In contrast, the isotherm at $T = 0.85$ does not permit an equal areas construction. This is because $T = 0.85$ lies below the temperature T^*, and therefore no unbending transition is possible. In each of the isotherm shown in Figure 4(a) the vertical dashed lines correspond to the respective locations of the pre-wetting transitions. We remark here that the present mean-field considerations will be altered when fluctuation effects are included, leading to the rounding of the first-order unbending transitions.

In Figure 5 we show coexisting profiles at three different temperatures along the unbending line for a wall with a stripe of width $L = 32$. Notice that as the temperature is decreased towards T^*, three things happen; the lateral extent of the dry region near the stripe (lower panel in each figure) grows, the height of the adsorbed liquid layer away from the patch increases, and finally the interface from the thin to thick phases sharpens. As the temperature is further decreased to T^*, the dry region nucleated at the stripe [lower panel in Figure 5(a)] grows continuously, consistently with complete pre-wetting discussed earlier.

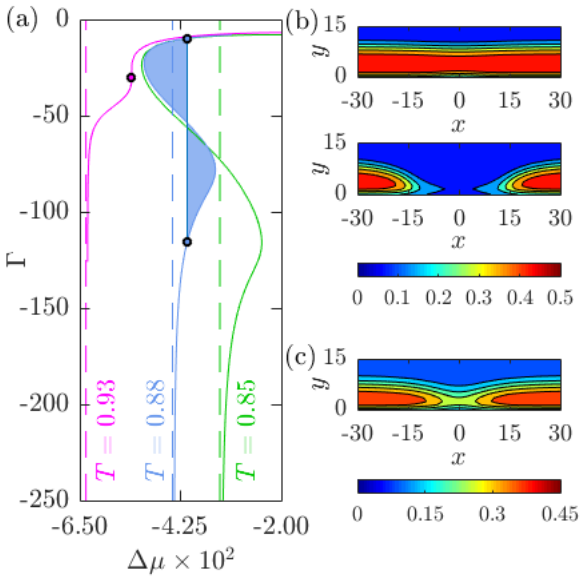

Figure 4. Representative adsorption isotherms at three different temperatures for a stripe of width $L = 8$. In figure (a) we illustrate the generalized Maxwell constructions for the unbending critical point occurring at $T = 0.93$, and an equal areas construction for the coexistence of different phases, at $T = 0.88$, corresponding to a first-order unbending (local surface condensation) phase transition. The corresponding unique and coexisting density profiles are shown in figures (c) and (b), respectively. In figure (a) we also show an isotherm for $T = 0.85$, which does exhibit an equal areas construction, meaning that there is no unbending transition. The vertical asymptotes of each isotherm correspond to the locations of the pre-wetting transitions, at $\Delta\mu_{\rm pw} = (-3.37, -4.43, -6.36) \times 10^{-2}$.

4. Conclusion

In this paper we have investigated the surface phase equilibria and criticality occurring on a planar wall decorated with a deep stripe of a weaker adsorbing (relatively solvophobic) material. Both materials would exhibit, as homogeneous walls, first-order transitions with corresponding pre-wetting lines. The surface phase diagram is with, one crucial exception, similar to that occurring when the stripe is solvophillic. Let us first summarise the similarities. The pre-wetting transition of the outer substrate remains a phase boundary and the order of the pre-wetting transition is changed to continuous when approached from the appropriate side. This reflects the scenario of 2D complete pre-wetting when either a thin or thick pre-wetting layer spreads away from the stripe. Similarly both phase diagrams show first-order unbending transitions corresponding to the local condensation/evaporation near the stripe. In both cases the line of unbending transitions can merge with the pre-wetting line at a temperature T^*, which corresponds to a 2D first-order wetting transition, and this temperature approaches the pre-wetting critical point as L is reduced.

There is however one major difference between the solvophillic and solvophobic scenarios. As mentioned in the introduction, when the stripe is solvophillic, the the unbending and pre-wetting lines only merge when L is sufficiently small [38]. For larger stripe widths the unbending and pre-wetting lines are distinct and as L increases the line of unbending transitions approaches the pre-wetting transition of the homogeneous striped phase as expected. This does not seem to case when the stripe is solvophobic when even for the largest stripe widths considered our computations indicate clearly

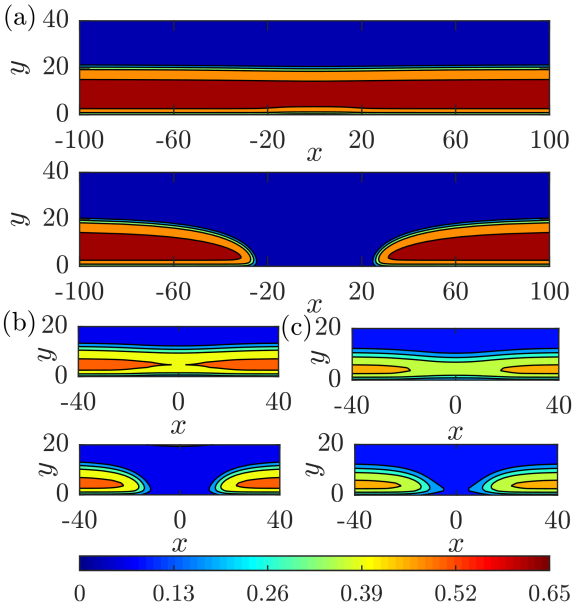

Figure 5. Representative coexisting configurations along the unbending line for a wall with a stripe of width $L = 32$. Panels (a) – (c) correspond to increasing temperatures $T = 0.76$, 0.88 and 0.92. The lower panel in each figure illustrates the extent of the thin gas-like coexisting phase, which spreads out away from the stripe. The extent of this drying layer increases as the temperature T is decreased towards $T^* \approx 0.75$.

that the unbending and pre-wetting lines still merge at a temperature T^*. Indeed preliminary results for even larger widths ($L = 64$) still show this merging with the value of T^* lying very close to , but above, T_w^w. Of course in the limit $L \to \infty$ the unbending line must coincide with the pre-wetting line of the inner striped phase. But our study indicates that this does not happen in the same, smooth manner as for the case of a solvophillic stripe. This is reminiscent of the phase equilbiria occurring in a parallel plate geometry with competing (one critically wetting, one critically drying) walls for which as the slit width L increases the line of phase coexistence ends at a critical temperature which tends towards the wetting temperature rather than the bulk critical temperature [13]. Similarly we conjecture that in the present case of a solvophobic stripe the temperature at which the unbending and pre-wetting lines merge T^* approaches the wetting temperature of the outer wall T_w^w as $L \to \infty$. This is very strongly suggested by the surface phase diagrams shown in Fig 2 where we observe that additionally for the largest stripe widths $L = 32$ the unbending critical point lies very close to the pre-wetting critical point of the inner (stripped) substrate. If this scenario is correct then there must be a reason why, for the solvophobic stripe, the line of unbending transitions must never touch the bulk saturation curve. For this we offer a tentative explanation. Imagine that similar to the solvophillic case at some sufficiently large L the unbending line detaches from the pre-wetting line. In that case it meets the bulk coexistence curve at some temperature lying above T_w^w. What would the coexisting phases look like at this temperature? The "thick" or unbent phase would correspond simply to the complete wetting of the entire substrate. The "thin" or bent state on the other hand must be locally dry near the stripe. This requires that the local height of liquid-gas interface each side of the patch increases from a microscopic

to a macroscopic value as we move away from the stripe. However for systems with dispersion forces the excess free-energy associated with this configuration diverges logarithmically as $\Delta\mu \to 0$, similar to the divergence of the line tension at first-order wetting [49] suggesting that such coexistence is strictly forbidden. No such diverging contribution to the free-energy occurs for the case of a solvophillic stripe since in that case neither coexisting phase has macroscopic adsorptions since the outer wall is still partially wet. This must mean that for very wide solvophobic stripes the unbending line would lie close to the pre-wetting line of the inner substrate, but breaks away from it, close to $T_w^{(s)}$ and runs along, but below, the bulk coexistence curve, meeting the lower pre-wetting line at a temperature $T^* \approx T_w^{(w)}$. This would be one mechanism by which the surface phase diagram converges to both pre-wetting lines as L becomes macroscopic.

Acknowledgement

PY acknowledges many discussions with Dr Miguel Dúran-Olivencia from Chemical Engineering Department at Imperial College London. We acknowledge financial support from the Engineering and Physical Sciences Research Council of the UK through Grants No. EP/L027186 and EP/L020564 and by the European Research Council through Advanced Grant No. 247031.

References

[1] J.W. Cahn, J. Chem. Phys. **66**, 3667 (1977).
[2] C. Ebner and W.F. Saam, Phys. Rev. Lett. **38**, 1486 (1977).
[3] D.E. Sullivan, Phys. Rev. B **20**, 3991 (1979).
[4] D.B. Abraham, Phys. Rev. Lett. **44**, 1165 (1980).
[5] E. Brézin, B.I. Halperin and S. Leibler, Phys. Rev. Lett. **50** (18), 1387–1390 (1983).
[6] R. Lipowsky and M.E. Fisher, Phys. Rev. B **36** (4), 2126–2141 (1987).
[7] A.O. Parry, J.M. Romero-Enrique and A. Lazarides, Phys. Rev. Lett. **93** (8), 086104 (2004).
[8] M. Schick, in *Les Houches 1988. Liquids at Interfaces.*, edited by J. Charvolin, J. F. Joanny and J. Zinn-Justin (, , 1990), p. 415.
[9] S. Dietrich, in *Phase Transitions and Critical Phenomena*, edited by C. Domb and J. L. Lebowitz, Vol. 12 (, , 1988), p. 2.
[10] G. Forgacs, R. Lipowsky and T.M. Nieuwenhuizen, in *Phase Transitions and Critical Phenomena*, edited by C. Domb and J. L. Lebowitz, Vol. 14 (, , 1991), p. 135.
[11] R. Evans, U.M.B. Marconi and P. Tarazona, J. Chem. Phys. **84**, 2376 (1986).
[12] R. Evans, U.M.B. Marconi and P. Tarazona, J. Chem. Soc. Faraday Trans. 2 **82**, 1763 (1986).
[13] A.O. Parry and R. Evans, Phys. Rev. Lett. **64** (4), 439–442 (1990).
[14] A.O. Parry and R. Evans, Physica A **181** (3), 250–296 (1992).
[15] R. Evans, Adv. Phys. **28**, 143 (1979).
[16] J.F. Lutsko, in *Adv. Chem. Phys.* (, , 2010), p. 1.
[17] K. Rejmer, S. Dietrich and M. Napiorkowski, Phys. Rev. E **60**, 4027 (1999).
[18] A.O. Parry, C. Rascón and A.J. Wood, Phys. Rev. Lett. **83**, 5535 (1999).
[19] A.O. Parry, C. Rascón and A.J. Wood, Phys. Rev. Lett. **85**, 345 (2000).
[20] A. Malijevsky and A.O. Parry, Phys. Rev. Lett. **110**, 166101 (2013).
[21] A.O. Parry, C. Rascón, N.B. Wilding and R. Evans, Phys. Rev. Lett. **98**, 226101 (2007).
[22] R. Roth and A.O. Parry, Mol. Phys. **109**, 1159 (2011).

[23] A.O. Parry, A. Malijevský and C. Rascón, Phys. Rev. Lett. **113** (14) (2014).
[24] C. Rascón, A.O. Parry, R. Nurnberg, A. Pozzato, M. Tormen, L. Bruschi and G. Mistura, J. Phys.: Condens. Matter **25**, 192101 (2013).
[25] A. Checco, B.M. Ocko, M. Tasinkevych and S. Dietrich, Phys. Rev. Lett. **109**, 166101 (2012).
[26] K. Binder, Annu. Rev. Mater. Res. **38**, 123 (2008).
[27] P. Yatsyshin, N. Savva and S. Kalliadasis, J. Chem. Phys. **142**, 034708 (2015).
[28] P. Yatsyshin, N. Savva and S. Kalliadasis, J. Phys.: Condens. Matter **27**, 275104 (2015).
[29] T.M. Squires and S. Quake, Rev. Mod. Phys. **77**, 977 (2005).
[30] M. Rauscher and S. Dietrich, Annu. Rev. Mater. Res. **38**, 143 (2008).
[31] M. Rauscher and S. Dietrich, Soft Matter **5**, 2997 (2009).
[32] Z. Gou and W. Liu, Plant. Sci. **172**, 1103 (2007).
[33] A. Calvo, B. Yameen, F.J. Williams, G.J.A.A. Soler-Illia and O. Azzaroni, J. Am. Chem. Soc. **131**, 10866 (2009).
[34] K.W. Schwarz and J. Tersoff, Phys. Rev. Lett. **102** (2009).
[35] R.E. Algra, M.A. Verheijen, L.F. Feiner, G.G.W. Immink, W.J.P. van Enckevort, E. Vlieg and E.P.A.M. Bakkers, Nano Lett. **11**, 1259 (2011).
[36] D. Lohse and X. Zhang, Rev. Mod. Phys. **87**, 981 (2015).
[37] C. Rascón and A.O. Parry, J. Chem. Phys. **115**, 5258 (2001).
[38] P. Yatsyshin, A.O. Parry, C. Rascón and S. Kalliadasis, J. Phys.: Condens. Matter **29**, 094001 (2017).
[39] W.F. Saam, J. Low Temp. Phys. **157**, 77 (2009).
[40] P. Yatsyshin, A.O. Parry and S. Kalliadasis, J. Phys.: Condens. Matter **28**, 275001 (2016).
[41] C. Bauer and S. Dietrich, Eur. Phys. J. B **10**, 767 (1999).
[42] C. Rascón and A.O. Parry, J. Phys.: Condens. Matter **12**, A369 (2000).
[43] C. Bauer and E. Dietrich, Phys. Rev. E **61**, 1664 (2000).
[44] P. Yatsyshin and S. Kalliadasis, Mol. Phys. **114**, 2688 (2016).
[45] J. Wu, AIChE J **52**, 1169 (2006).
[46] J. Landers, J. Yu. Gor and A.V. Neimark, Colloid. Surf. A **437**, 3 (2013).
[47] J.A. Barker and D. Henderson, J. Chem. Phys. **47**, 4714 (1967).
[48] P. Yatsyshin, N. Savva and S. Kalliadasis, J. Chem. Phys. **136**, 124113 (2012).
[49] J.O. Indekeu, Physica A **183** (4), 439–461 (1992).